STUDY ON SEISMIC LATERALE STRENGTH OF COUPLED BATTERED STEEL PIPE PILE

Shoichi Nakatani[1], Masahiro Takeguchi[2], Hisataka Iochi[3], Norihiko Suzuki[4]

ABSTRACT

A battered pipe pile foundation has excellent sustaining capacity for horizontal loads. However the seismic lateral strength and ductility of the battered pile under a large horizontal load have not yet been clarified for highway bridge foundation in Japan. In the present study, loading tests for coupled battered piles are performed, and seismic lateral strength and ductility is evaluated in comparison with the previous tests for coupled vertical piles. As a result, it was verified that coupled battered piles have larger lateral stiffness than coupled vertical piles at the initial loading stage, and the maximum strength of coupled battered piles is larger than that of coupled vertical piles. In addition, if the allowable displacement for the lateral strength is evaluated as the displacement at maximum strength δ_{Pmax} , ductility factor $\mu = 4.5 – 5.0$ is evaluated.

INSTRUCTION

A battered pipe pile foundation has excellent sustaining capacity for horizontal loads, especially for a bridge abutment foundation on soft ground. In addition, in the case of the lateral movement of the abutment, a battered pile foundation is evaluated as a more rigid foundation than the vertical pile foundation. A battered pile used to be installed with a driving hammer, but the driving hammer has been prohibited to prevent noise and vibration since the 1980s in Japan. So the battered pile has not been applied to bridge foundations. Recently, new pile installation methods such as the screwed pile that can be installed with low noise and low vibration has been developed. Thus, by using these methods, the battered pile can be applied to bridge foundations.

The seismic design of highway bridge foundations in Japan was modified so as to prevent collapse due to rare large earthquakes. In order to meet the seismic design rules, the lateral strength of vertical pile foundations for large seismic loads was performed by loading model tests for the coupled vertical piles at the Public Works Research Institute in 1996[1),2)]. However the seismic lateral strength and ductility of the battered pile under a large horizontal load have not yet been clarified. This report presents an evaluation of the lateral strength and ductility of coupled battered piles of a bridge foundation by loading model tests in the air (not on the ground) compared with previous tests of coupled vertical piles [3),4)]. The relationship between horizontal load and displacement and the allowable design ductility factor of the coupled battered piles are also studied.

[1] Team Leader, Foundation Engineering Research Team, Public Works Research Institute
[2] Senior Researcher, ditto
[3] Collaborating Researcher, ditto
[4] Technical Member, Japanese Association for Steel Pipe Piles

LOADING MODEL TEST

The models of the test are shown in Figure 1. Loading tests were planned for two types of model, 2 lines x 3 piles (3-pile model) and 1 line x 4 piles (4-pile model). These models have two battered piles (8-degree inclination) at both edges of the piles. The footings (upper and lower) are firmly connected to the piles by inserting 1D (diameter).

The steel pipe of the test model has same properties as the previous tests for coupled vertical piles as shown in Table 1. The result of the tension test for the steel pipe is shown in Table 2. In addition, the results of the compression test for the concrete of the footing and the filled concrete in the pile ends are shown in Table 3.

The experimental set-up is shown in Figure 2. The test models were laid on the test floor because of the loading jack position. Alternate horizontal loads were applied to the upper footing at a height of 1500 mm above the pile top and fixed vertical loads were applied on the top of the upper footing during the loading test. The vertical load and expected maximum horizontal loads are shown in Table 4. The alternate load step was shown in Figure 3. Basic displacement $1\delta_y$ is determined as the displacement when the stress of the all piles reaches its yield by a nonlinear calculation.

The items of measurement and measuring devices are shown in Table 5.

TEST RESULTS

A photograph of the experimental set-up is shown in Photo 1.

[3-pile model]

At $1\delta_y$, the strain at both ends (upper and lower) of the battered piles becomes greater than the actual yield strain as calculated. At $2\delta_y$ the strain at both ends of all piles becomes greater than the actual yield strain, and small local buckling at both ends of the battered piles occurs. At $3\delta_y$, local buckling develops and remains during opposite direction loading (minus horizontal loading). At $4\delta_y$, local buckling develops as elephant foot buckling and local buckling at the center pile is observed. However, a decrease in strength does not occur. At $5\delta_y$, several fissures in the concrete of the upper footing are observed. At the second cycle, a decrease in strength occurs.

[4-pile model]

At $1\delta_y$, the strain at both ends (upper and lower) of the battered piles becomes greater than the actual yield strain same as in the case of 3-pile model. At $2\delta_y$ the strain at both ends of all piles becomes greater than the actual yield strain and small local buckling at both ends of the battered piles does not occur. At $3\delta_y$, small local buckling is observed. At $4\delta_y$, local buckling at both ends of the battered piles is observed and several fissures in the concrete of both footings (upper and lower) are observed. However, a decrease in strength does not occur (Photo 2). At $5\delta_y$, local buckling at the center pile is observed. At the second cycle of $6\delta_y$, a decrease in strength occurs.

From the loading tests of coupled battered piles, it is found as follows:

1) Firstly, on the battered pile, plastic hinges at the pile top and the pile in the ground are generated.
2) Secondly, on the center pile (vertical pile), plastic hinges and a decrease in strength is generated.

The relationship between horizontal load and displacement for the 3-pile model and 4-pile model are shown in Figure 4 and Figure 5, respectively. From these figures, it is found as follows:

1) Horizontal load - displacement curves are shown as symmetrical in both directions of loading. The loading tests are performed successfully.
2) Horizontal load – displacement loops are shown as spindle shaped. It shows that the energy absorption of the coupled battered piles is relatively large.
3) Maximum strength is observed at $4\delta_y$.

COMPARISION BETWEEN VERTICAL PILES AND BATTERED PILES

Comparison between the test result of the coupled battered piles and that of the coupled vertical piles performed in 1996 is shown in Figure 6 (3-pile model) and Figure 7 (4-pile model). The previous test of coupled vertical piles (4-pile model) was conducted for a 2-line x 4-pile model, so the horizontal load is reduced to half in the figure. The comparison shows as follows:

1) At the initial loading stage, coupled battered piles have larger lateral stiffness than coupled vertical piles.
2) In the case of the 3-pile model, the maximum strength of coupled battered piles is 30% larger than that of coupled vertical piles; however, the displacement at the maximum strength of coupled battered piles is 30% smaller than that of coupled vertical piles.
3) Also in case of the 4-pile model, the maximum strength of coupled battered piles is 20% larger than that of coupled vertical piles; however, the displacement at the maximum strength of coupled battered piles is 60% smaller than that of coupled vertical piles.
4) The maximum strength of coupled battered piles depends on the rate of battered pile existing in the piles (nos. of battered piles / total nos. of piles).

Comparison between the test result and the design strength curve determined by nonlinear analysis is shown in Figure 8 (3-pile model) and Figure 9 (4-pile model). The design strength curve is calculated by using push-over analysis as follows:

a) Both footings are modeled as a rigid frame;
b) The connection between the pile and the footing is modeled as rigid;
c) The M-φ relationship is modeled as bilinear.

From Figure 8 and Figure 9, the lateral strength of the test results within a displacement of $\pm 5\delta_y$ is larger than the design strength curve, and coupled battered piles have excellent lateral strength and ductility.

The ductility factor is determined by using Energy Conservation Principle to the enveloping curve of the maximum loads of the tests. The schema of Energy Conservation Principle is shown in Figure 10.By using Energy Conservation Principle in which energy absorption for area (A+B) is equivalent to that for area (A'+B), the equivalent displacement δ_E is determined, and ductility factor μ is calculated as shown below:

$$\mu = \delta_E / \delta_{y'} \quad (1)$$

Yield displacement $\delta_{y'}$ is determined as the point of sharp increase for horizontal displacement. The allowable displacement for the lateral strength is evaluated as two cases: 1) the displacement at maximum strength δ_{Pmax} , and 2) maximum displacement δ_{max}.

Ductility factor μ is 4.5 – 8.5 as shown in Table 6. If the allowable displacement for the lateral strength is evaluated as the displacement at maximum strength δ_{Pmax} , ductility factor μ = 4.5 – 5.0 is evaluated.

CONCLUSION

In the present study, loading tests for coupled battered piles are performed, and seismic lateral strength and ductility is evaluated in comparison with the previous tests for coupled vertical piles. The main conclusion is given as follows:

(1) Coupled battered piles of bridge foundations have larger lateral strength than vertical battered piles, and the decrease in strength is evaluated as slow because of efficient ductility.

(2) In the case of the same numbers of piles, coupled battered piles have larger lateral stiffness than coupled vertical piles at the initial loading stage, and the maximum strength of coupled battered piles is larger than that of coupled vertical piles.

(3) The maximum strength of coupled battered piles depends on the rate of battered pile existing in the piles (nos. of battered piles / total nos. of piles).

(4) Maximum strength is observed at $4\delta_y$. The lateral strength of the test results within a displacement of $\pm 5\delta_y$ is larger than the design strength curve, and coupled battered piles have excellent lateral strength and ductility.

(5)If the allowable displacement for the lateral strength is evaluated as the displacement at maximum strength δ_{Pmax} , ductility factor μ = 4.5 – 5.0 is evaluated.

In the actual bridge foundations, horizontal stiffness, maximum strength, and the ductility of coupled battered piles depend on the ground condition, inclination of the battered pile, and the rate of battered pile in the piles. These studies, as well as studies on the behavior of battered pile under subsidence of soft ground, will be continuously performed.

Part of this study was subsidized by JISF (The Japan Iron and Steel Federation).

REFERENCES

1) Nakano, Kimura, Isizawa, Simazu, Oyama, Horizontal loading model test for steel pipe pile foundation(No.1), 32th Conference on Japan Geotechnical Engineering, pp.1573-1574, 1997,7

2) Fukui, Kimura, Yosida, Suzuki, Hirata, Horizontal loading model test for steel pipe pile foundation(No.2), 32th Conference on Japan Geotechnical Engineering, pp.1575-1576, 1997,7
3) Iochi, Nakatani, Takeguchi, Okahara, Komatsu, Hirata, Takano, Ikeda, Takahashi, Study on Horizontal Bearing Capacity of Coupled Battered Steel Pipe Pile(No.1), 41th Conference on Japan Geotechnical Engineering, pp.1385-1386, 2006,7
4) Iochi, Nakatani, Takeguchi, Okahara, Komatsu, Hirata, Takano, Ikeda, Takahashi, Study on Horizontal Bearing Capacity of Coupled Battered Steel Pipe Pile(No.2), 41th Conference on Japan Geotechnical Engineering, pp.1387-1388, 2006,7

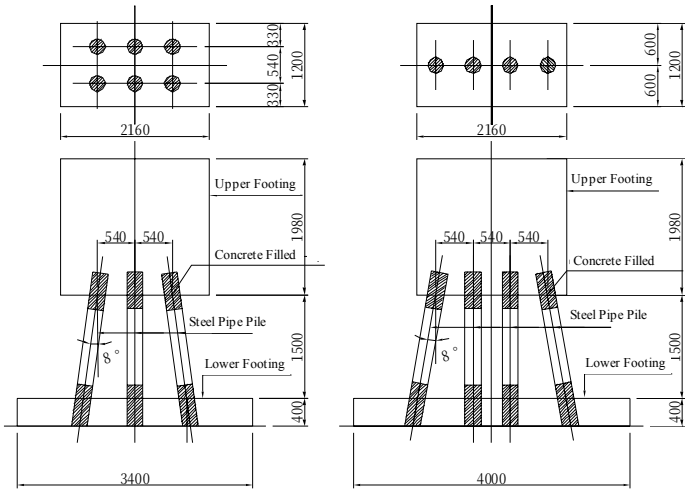

(1) 3 Pile Model (2) 4 Pile Model

Fig.1 Outline of Test Models

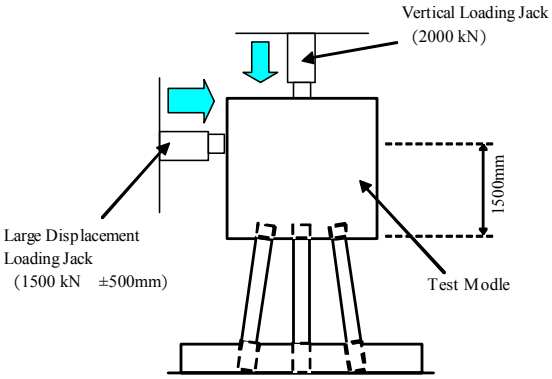

Fig.2 Apparatus for Loading Test

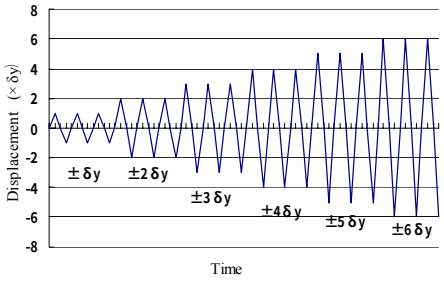

Fig.3 Alternate Loading Steps

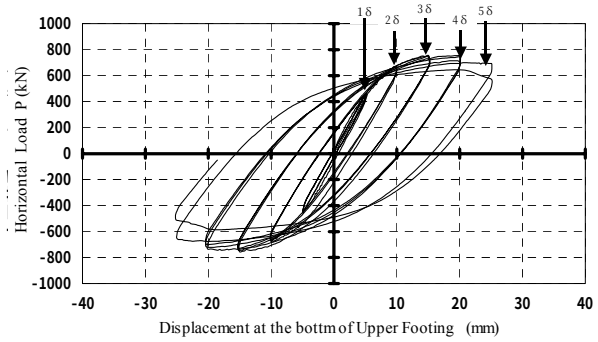

Fig.4 Relation between Horizontal Load and Displacement (3 Pile Model)

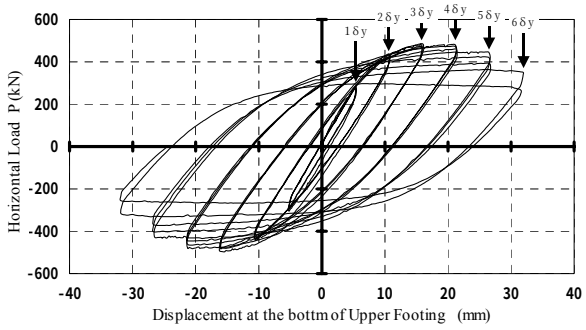

Fig.5 Relation between Horizontal Load and Displacement (4 Pile Model)

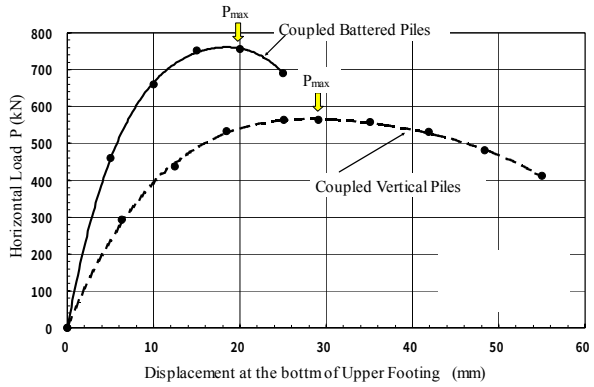

Fig.6 Enveloping Curves of Maximum Loads for Vertical Piles and Battered Piles (3 Piles Model)

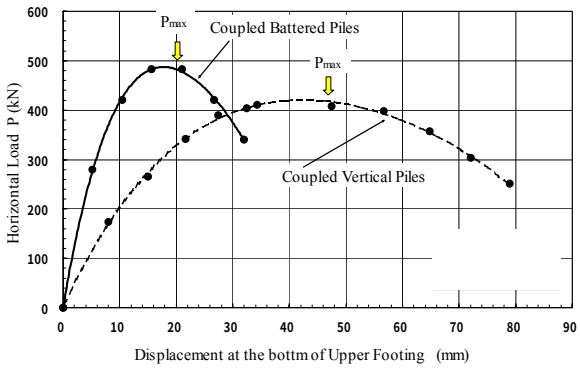

Fig.7 Enveloping Curves of Maximum Loads for Vertical Piles and Battered Piles (4 Pile Model)

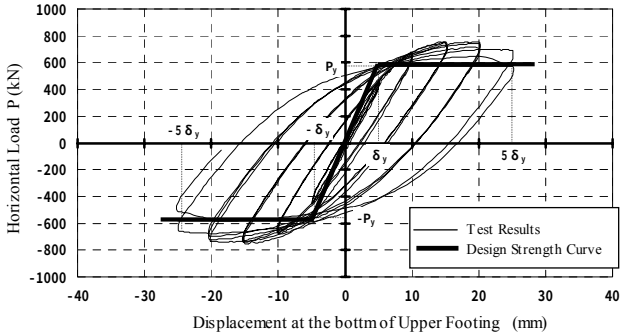

Fig.8 Comparison between Test Results and Design Resistance Curve (3 Pile Model)

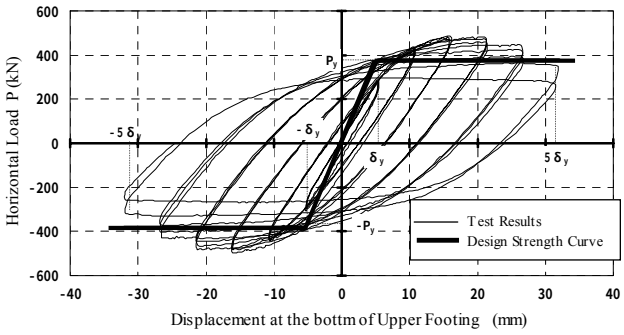

Fig.9 Comparison between Test Results and Design Resistance Curve (4 Pile Model)

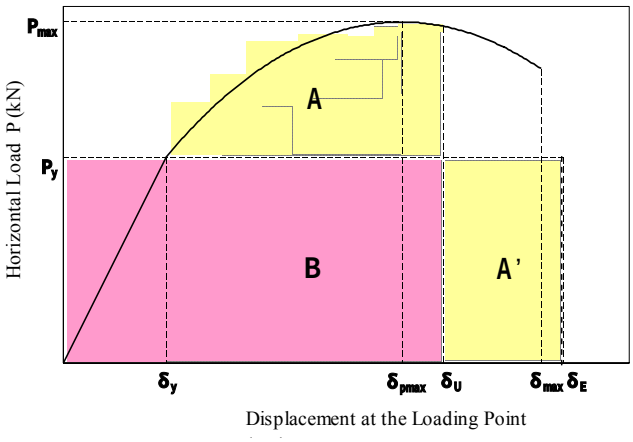

Fig.10 Schema of Energy Conservation Principle

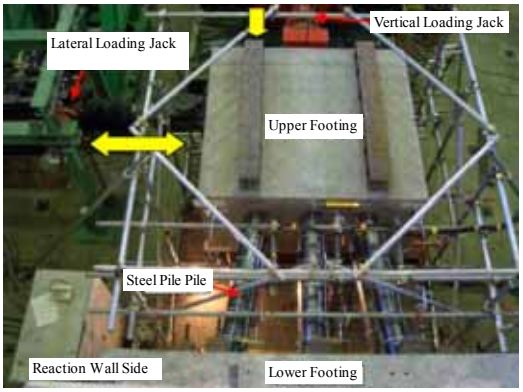

Poto.1 Experimental Set-up

Poto.2 Final Deformation of Pile Head

Table 1 Dimension of Pipe Pile

No.	Model Type	Diameter (mm)	Thickness (mm)	Pipe SPEC.	Notes
1	3 Pile Model	216.3	4.2	STK400	1 D (Diameter) Filled with Concrete from Both Edges.
2	4 Pile Model				

Table 2 Tensile Test Results of Pipe Pile

	0.2%Strength (N/mm^2)	Elastic Modulas (kN/mm^2)	Elongation (%)
Average	350.1	214.3	37.7

Table 3 Compressive Strength Test Results of Concrete

	Strength (N/mm^2)	Density (kg/m^3)
Footing	77.21	2.358
Filling（Upper）	34.67	2.324
Filling（Lower）	34.15	2.275

Table 4 Vertical Load and Maximum Assumption of Horizontal Load

Model Type	Numbers of Pile	Vertical Load (Fixed)	Horizontal Load (Maximum Assumption)
3 Pile Model	6本	900kN	1,200kN
4 Pile Model	4本	600kN	800kN

Table 5 Measurement Items and Device

Measurement Items	Device	Numbers of Measurement Point	
		3 Pile Model	4 Pile Model
(1) Vertical Load	Load Cell	1	1
(2)Horizontal Load	Load Cell	1	1
(3) Displacement			
Vertical Jack	Stroke	1	1
Horizontal Jack	Stroke	1	1
Upper Footing(H)	Displacement Meter	8	8
Upper Footing(V)	Displacement Meter	8	8
Lower Footing(H)	Displacement Meter	2	2
Lower Footing(V)	Displacement Meter	4	4
Pile	Displacement Meter	9	12
(4) Strain of Pile	Strain Gauge	168	112
(5) Pile Buckling	Shape Gauge	—	—

Table 6 Calculation Results of Ductility factor

Items	3 Pile Model		4 Pile Model	
	$\delta_U=\delta_{Pmax}$	$\delta_U=\delta_{max}$	$\delta_U=\delta_{Pmax}$	$\delta_U=\delta_{max}$
Yielding Disp. δ_y (mm)	6.4		5.9	
Yielding Load P_y (mm)	461.6		280.2	
Displacement at Maximum Strength δ_{Pmax} (mm)	23.6		19.6	
Maximum Load Pmax (kN)	755.5		486.0	
Maximum Disp. δ_{max} (mm)	29.5		35.1	
Equivalent Disp. δ_E (mm)	31.4	41.5	26.2	50.2
Ductility factor μ	5.0	6.5	4.5	8.5